Supporting Information

Short et al. 10.1073/pnas.0910921107

SI Text

Empirical Crime Data. The reaction-diffusion model described by Eqs. **1** and **2** is based on empirical evidence for how offenders move and mix with potential targets and how targets/victims of crime appear to respond to offender attacks under a wide range of crime types. Data on single-family residential burglary, provided to us by the Long Beach Police Department, Long Beach, California, illustrate the phenomena of repeat victimization, near-repeat victimization, and journey-to-crime distances.

Raw burglary data were scrubbed for duplicates and the remaining events were geocoded using ESRI's ArcGIS platform. Nearly 98% of events were successfully address-matched yielding a total sample of 9,042 geocoded single-family residential burglaries reported within the city of Long Beach in 2000–2005. For each of these crimes we possess information on the geographic location of the event and day that the crime was reported.

Of the 9,042 events, 7,002 are houses that were victimized exactly once, 819 are houses victimized exactly twice, 98 victimized exactly three times, and 25 are houses that were victimized four or more times. For analysis, we divided the dataset into six nonoverlapping 364 days sets and isolated all those houses that were victimized exactly two times within a given set. We then calculated the time interval τ in days between the first and second burglaries for each of these residences (1). The frequencies of observed time intervals were normalized to give an empirical probability distribution $p_2(\tau)$. This empirical distribution is compared to the theoretical expectation for repeat burglaries occurring as the result of a time-invariant Poisson process (Fig. 1*A*). Deviations from the Poisson expectation indicate that short repeat time intervals are more common than expected from independent burglary events, while long repeat intervals are therefor less common. We interpret this as evidence that initial burglaries generate an enhanced risk that pulls offenders back to that location to commit a repeat crime. The elevated risk lasts for approximately six weeks in the Long Beach data, from which we infer that risk eventually decays back to a baseline environmental level.

To examine whether the enhanced risk following an initial burglary also diffuses to neighbors, we isolated those houses in the Long Beach dataset that were victimized exactly once within any of the six time windows mentioned above. For each of these houses, we measured the distance in meters to all other such houses in the same time window, along with the time separation τ between the two events. For varying distance bands, we then determined the fraction of time intervals that were less than or equal to 14 days. This observed fraction is plotted as a function of distance between the two homes and compared to an expected fraction of near-repeat burglaries assuming a Poisson process, which is independent of physical separation (Fig. 1*B*). Deviations above the Poisson expectation for nearby homes indicate that burglaries are temporally and spatially correlated with one another. We explain this correlation as the diffusion of risk from a focal burglary to nearby houses. Enhanced risk diffuses as far as ∼2000 m, at which point the frequency of burglary near-repeats follows a Poisson expectation for independent events.

We suppose that offenders are primarily responsible for spreading enhanced crime risk. A spatial limit of ∼2000 m for the diffusion of crime risk suggests that offenders primarily search locally for targets. We corroborate this observation with journey-to-crime distances for residential burglars committing crimes in Long Beach, California. Between 2000–2005, the Long Beach Police Department linked 857 residential burglaries to criminal suspects or arrestees for which a home location is known. The number of suspects and arrestees represents ∼9.5% of all residential burglaries, which is consistent with burglary clearance rates of ∼12% for the United States (2), given that our count includes only those offenders with known residential addresses. For each of the 857 burglaries, we calculated the linear distance in km between the known home location for the offender and the crime location. We excluded eight burglaries that showed a distance of zero km between offender residence and crime location. There is at least one instance in the dataset for all distances between 1 and 32 km, representing 97.3% of all observed search distances > 0 km. Beyond 32 km the data are clearly sparse and the maximum observed journey-to-crime distance is 163 km. The mean and standard deviation in journey-to-crime distances for the continuous portion of the curve between 1 and 32 km are 4.95 km and 6.16 km, respectively. Fig. 1*C* gives the raw frequency histogram for journey-to-crime distances < 15 km. Observed journey-to-crime distances are typically short, suggesting that local search predominates in offender behavioral routines [(3), but see Ref. 4].

Methods. The PDE model is integrated using a semiimplicit spectral method (5), typically on a square lattice containing 128×128 nodes and using periodic boundary conditions.

The linear stability analysis of Eqs. **1** and **2** is accomplished by assuming a solution for each that is the homogeneous steady value plus a perturbation of the system taking the form of a small amplitude sine wave with wavelength $\lambda = 2\pi/k$ and exponential growth (or decay) rate σ:

$$A(x,t) = \bar{A} + \delta_A e^{\sigma t} e^{ikx}, \qquad \rho(x,t) = \bar{\rho} + \delta_\rho e^{\sigma t} e^{ikx}.$$

These solutions are substituted into the equations, any terms that are nonlinear in the small amplitudes are ignored, and the growth rate σ is then determined as a function of λ. Those wavelengths with positive growth rates are unstable, and those with negative growth rates are stable; the parameters of the system determine which, if any, of the wavelengths fall into each category.

Linear stability analysis provides only an indication of when linear instabilities may nucleate into hotspots, since all nonlinear terms are discarded. Our weakly nonlinear analysis explicitly examines the behavior of the nonlinear terms resulting from system perturbation, allowing us to discover the existence of large intensity, stable hotspots in the linearly stable regime (the so-called subcritical hotspots), and establishes an approximate solution for the amplitude $A(\infty)$ describing steady-state hotspot intensity and geometry. We then confirm these findings by numerically solving the steady-state versions of Eqs. **1** and **2** in a radially symmetric geometry using a Newton-Raphson-based relaxation method and Neumann boundary conditions (Fig. 3*A*). The boundary between parameter regimes supporting supercritical and subcritical hotspot formation (Fig. 3*B*) is also determined numerically using bifurcation diagrams found for systems with varying values of ηA^0.

Hotspot suppression is modeled by instantaneously defining a "dampening field" $d(\mathbf{x})$ such that $d(\mathbf{x})$ is effectively equal to one in regions not currently within a hotspot and zero in regions that are within a hotspot; the value of $d(\mathbf{x})$ varies smoothly but rapidly between the two extremes on the hotspot edges. In both Eqs. **1** and **2**, the term ρA is replaced by $d\rho A$, so that no crime may occur in the dampened areas. After a set amount of time has passed, a new $d(\mathbf{x})$ field is determined using the current location of hotspots, if any.

1. Short MB, D'Orsogna MR, Brantingham PJ, and Tita G (2009) Measuring and modeling repeat and near-repeat burglary effects. *J Quant Criminol* 25:325–339.
2. Federal Bureau of Investigation (multiple editions) Crime in the United States, Uniform Crime Reports. in http://www.fbi.gov/ucr/ucr.htm.
3. Rengert GF, Piquero AR, and Jones PR (1999) Distance decay reexamined. *Criminology* 37(2):427–445.
4. Van Koppen P and De Keijser J (1997) Desisting distance decay: On the aggregation of individual crime trips. *Criminology* 35:505.
5. Short MB, et al. (2008) A Statistical Model of Criminal Behavior. *Math Models Methods Appl Sci* 18:1249–1267.

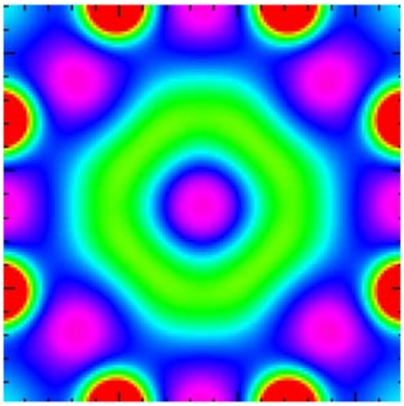

Movie S1. Hotspot displacement animation. Supercritical hotspots form under linearly unstable regimes. Nonlinear analysis suggests that suppression of supercritical hotspots will lead to displacement of the hottest areas of crime into a ring. Numerical integration supports this finding and shows further that crime hotspots displaced into a ring quickly break up to form new hotspots located midway between hotspots being suppressed. Video animations illustrate the 2D effect of displacement of suppressed supercritical hotspots. A 1D cross-section shows how the central hotspot is displaced into adjacent locations.

Movie S1 (GIF)

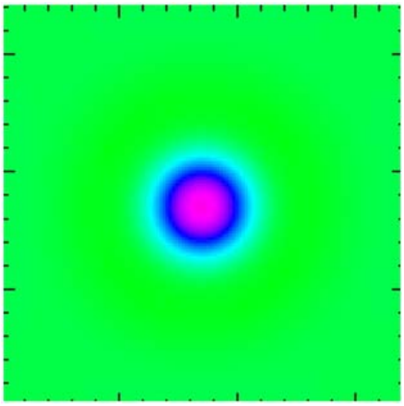

Movie S2. Hotspot dissipation animation. Subcritical hotspots form under linearly stable regimes with parameterizations close to unstable regimes. Nonlinear analysis suggests that suppression of subcritical hotspots will lead to dissipation of the hotspot, a phenomenon we describe as a hysteresis effect. Numerical integration supports this finding, showing that the locations of former hotspots during suppression actually have lower crime than surrounding regions. However, when suppression is removed crime within the former hotspot rebounds only to the environmental average. Hotspots will not reemerge unless a large enough spike in crime overrides the linear stability of the system.

Movie S2 (GIF)